DOI: 10.1002/chem.200600132

Peculiarities of $C_{60}^{\bullet -}$ Coordination to Cobalt(II) Octaethylporphyrin in Ionic Multicomponent Complexes: Observation of the Reversible Formation of Co−C(C_{60}^{-}) Coordination Bonds

Dmitri V. Konarev,*[a, b] Salavat S. Khasanov,[a, c] Akihiro Otsuka,[d] Gunzi Saito,*[a] and Rimma N. Lyubovskaya[b]

Abstract: Ionic multicomponent complexes containing the C_{60}^{-} anion, cobalt(II) octaethylporphyrin (OEP), and the noncoordinating tetramethylphosphonium cation (TMP^+), [(TMP^+){Co^{II}OEP(C_{60}^{-})}(C_6H_5CN)$_x$($C_6H_4Cl_2$)$_{1-x}$] ($x \cong 0.75$) (**1**), or the coordinating cation of *N*-methyldiazabicyclooctane ($MDABCO^+$), [{($MDABCO^+$)Co^{II}OEP(C_{60}^{-})}(C_6H_5CN)$_x$($C_6H_4Cl_2$)$_{1-x}$] ($x \cong 0.67$) (**2**), were obtained. Diamagnetic σ-bonded {Co^{II}OEP(C_{60}^{-})} units in **1** have the Co···C(C_{60}^{-}) distance of 2.268(1) Å at 100 K and are stable up to 290 K. Both $MDABCO^+$ and C_{60}^{-} coordinate to Co^{II}OEP in **2**. In this case, a noticeably longer Co···C(C_{60}^{-}) distance of 2.508(4) Å was observed at 100 K. As a result, the unprecedented reversible formation of the Co−C(C_{60}^{-}) coordination σ bond is realized in **2** and is accompanied by a transition from a paramagnetic to a diamagnetic state in the 50–250 K range. It was shown, for the first time, that the Co···C distance of about 2.51 Å is a boundary distance below which the Co−C(C_{60}^{-}) coordination bond is formed.

Keywords: crystal engineering · donor–acceptor systems · fullerenes · porphyrinoids · solid-state structures

Introduction

Fullerene compounds with porphyrins and metalloporphyrins attract special attention because of their possible use as precursors for photovoltaic materials and models of artificial photosynthesis.[1,2] Fullerenes were shown to cocrystallize with metal octaethyl- and tetraarylporphyrins.[3–7] For some of these cocrystals, weak metal–carbon(fullerene) bonding was found. For example, cobalt(II) octaethylporphyrin (Co^{II}OEP), cobalt(II) tetraphenylporphyrin (Co^{II}TPP), and iron(III) tetraphenylporphyrin form complexes with C_{60} with M···C(C_{60}) contacts with lengths of 2.67–2.71, 2.63–3.11, and 2.69–2.70 Å, respectively.[3–6] These contacts are noticeably shorter than the sum of the van der Waals radii of metal (M) and C atoms (>3.1 Å), but are essentially longer than the length of a strong M−C bond, for example, in alkylcobalamins (1.99–2.03 Å[8]). Nevertheless, this bonding orders the fullerene molecules in the complexes with metal octaethylporphyrins, and allows the molecular structures of some fullerene derivatives and endometallofullerenes to be studied.[3,9,10] Essentially stronger bonding between Co^{II}TPP and fullerene anions was observed in ionic multicomponent complexes, such as [{Cr^{I}(C_6H_6)$_2^{\bullet +}$}{Co^{II}TPP(fullerene$^-$)}$C_6H_4Cl_2$] (Cr(C_6H_6)$_2$ = bis(benzene)chromium; fullerene = C_{60} and $C_{60}(CN)_2$) with the lengths of the Co···C(fullerene$^-$) contacts being 2.28–2.32 Å. The coordination is realized by σ-type bonding, and most probably involves both electrons from the Co^{II}TPP d_{z^2} orbital and the LUMO of C_{60}^{-}. The resulting {Co^{II}TPP(fullerene$^-$)} coordination units are diamagnetic.[11] The Co···C(C_{60}^{-}) σ bonds are still relatively weak com-

[a] Dr. D. V. Konarev, Dr. S. S. Khasanov, Prof. G. Saito
Division of Chemistry, Graduate School of Science
Kyoto University, Sakyo-ku, Kyoto 606-8502 (Japan)
Fax: (+81) 75-753-40-35
E-mail: konarev@icp.ac.ru
saito@kuchem.kyoto-u.ac.jp

[b] Dr. D. V. Konarev, Prof. R. N. Lyubovskaya
Institute of Problems of Chemical Physics RAS
Chernogolovka, Moscow region 142432 (Russia)
Fax: (+7) 496-515-54-20

[c] Dr. S. S. Khasanov
Institute of Solid State Physics RAS
Chernogolovka, Moscow region 142432 (Russia)

[d] Dr. A. Otsuka
Research Center for Low Temperature and Materials Sciences
Kyoto University, Sakyo-ku, Kyoto 606-8502 (Japan)

Supporting information (IR and EPR data for complexes **1** and **2**; Table S1 and Figures S1–S4) for this article is available on the WWW under http://www.chemeurj.org/ or from the author.

pared with the strong Co–C bonds in alkylcobalamins, and their dissociation is possible. The changes in the degree of Co–C bonding can be monitored by using electron paramagnetic resonance (EPR) and superconducting quantum interference device (SQUID) techniques because two paramagnetic species are formed as a result of the dissociation. Complexes showing such dissociation can be interesting not only because of the reversible changes in their magnetic, conducting, and optical properties, but also because they can help to solve some fundamental problems of coordination and materials chemistries, one of which is how coordination bonds are formed and what limiting distances exist for such bonding. In $[(TDAE^{\bullet+})\{Co^{II}TPP(C_{60}^{-})\}]$ (TDAE = tetrakis(dimethylamino)ethylene), partial dissociation of the σ-bonded diamagnetic $\{Co^{II}TPP(C_{60}^{-})\}$ units is realized above 190 K and about 20% of the units dissociate at 290 K to form nonbonded paramagnetic Co^{II}TPP and $C_{60}^{\bullet-}$ species. As a result, the magnetic moment of the complex increases and the EPR signal broadens and shifts to larger *g*-factor values.[12] However, the crystal structure of this complex is unknown and therefore prevents a study of the structural aspects of such reversible coordination. An important task of materials chemistry is the development of new methods for modifying the physical properties of compounds, and in this work we will demonstrate how a simple variation of the countercations can drastically affect the properties of the resulting complexes.

In the present work, the crystals of two ionic multicomponent complexes, $[(TMP^{+})\{Co^{II}OEP(C_{60}^{-})\}(C_6H_5CN)_x(C_6H_4Cl_2)_{1-x}]$ ($x \cong 0.75$) (**1**) and $[\{(MDABCO^{+})Co^{II}OEP(C_{60}^{-})\}(C_6H_5CN)_x(C_6H_4Cl_2)_{1-x}]$ ($x \cong 0.67$) (**2**) (TMP^{+} = tetramethylphosphonium cation and $MDABCO^{+}$ = cation of *N*-methyldiazobicyclooctane), were obtained by means of diffusion. This has allowed us, for the first time, to study the molecular structures and properties of the new and unusual coordination $\{Co^{II}OEP{-}(C_{60}^{-})\}$ assemblies and observe the reversible formation of the $Co{-}C(C_{60}^{-})$ coordination bonds.

Results and Discussion

The selective reduction of C_{60} by propanethiol in the presence of potassium carbonate has been carried out in polar DMSO and a DMSO/benzene mixture up to the −2 and −1 charged states of C_{60}, respectively.[13] Recently, commercially available CH_3CH_2SNa has been used for the selective production of C_{60}^{2-} in acetonitrile.[14] Stirring a solution of C_{60} in a less-polar *o*-dichlorobenzene/benzonitrile ($C_6H_4Cl_2$/C_6H_5CN, 19:1) mixture with a tenfold molar excess of CH_3CH_2SNa at 60°C provided selective reduction of C_{60} to $C_{60}^{\bullet-}$ radical anions according to the near-IR (NIR) spectrum of the solution. However, the reduction takes a relatively long time (more than 6 h), and because of the poor solubility of the sodium salt of C_{60}, it partially precipitates from solution. The addition of a fivefold molar excess of any organic $(R^{+})(Hal^{-})$ salt (Hal = halide; in this work, we used MDABCOI and TMPCl) in the reaction mixture decreased the reduction time to less than one hour. NaI and NaCl did not dissolve in the solvents used and precipitated, thus allowing the reaction of cationic metathesis to be realized during the fullerene reduction. CH_3CH_2SNa and MDABCOI or TMPCl were also barely soluble in these solvents, and the excess of these salts was separated from the resulting solution by using filtration. $(R^{+})(C_{60}^{\bullet-})$ salts are soluble in the solvents used here and could be further crystallized by the diffusion of hexane. The crystallization of these salts in the presence of Co^{II}OEP afforded multicomponent complexes **1** and **2** whose compositions were determined from elemental analysis and verified by using X-ray diffraction on single crystals.

Both complexes have similar crystal structures at 100 K. The main building blocks of **1** and **2** are shown in Figure 1.

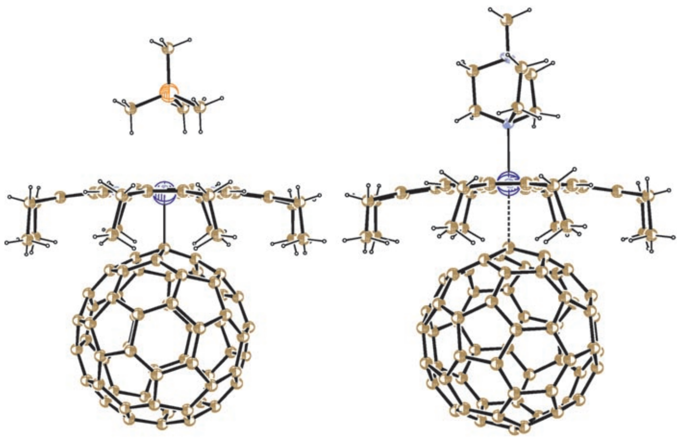

Figure 1. Molecular structures of the σ-bonded $\{Co^{II}OEP(C_{60}^{-})\}$ unit in **1** (left) and the $\{(MDABCO^{+})Co^{II}OEP(C_{60}^{-})\}$ assembly in **2** (right). Only the major orientation for disordered C_{60}^{-} is shown for **1** and **2** and one orientation of disordered $MDABCO^{+}$ is shown for **2**.

The cations and the fullerene anions are positioned on opposite sides of the Co^{II}OEP macrocycle. All eight ethyl groups of Co^{II}OEP are directed towards the fullerene to form a bowl-shaped conformation, which corresponds well with the spherical shape of C_{60}. There is one short Co···C(C_{60}^{-}) contact length of 2.268(1) Å in **1** indicating the formation of a σ bond between Co^{II}OEP and C_{60}^{-}. The distances between the Co atom and the carbon atoms closest to the coordinated carbon are longer (2.956–3.061 Å). The Co atom is shifted by 0.105(1) Å from the mean plane of the four nitrogen atoms towards the fullerene (the porphyrin macrocycle has a slightly concave conformation with a root mean square (rms) deviation of 0.090 Å). Previously described σ-bonded $\{Co^{II}TPP(fullerene^{-})\}$ anions have close Co···C(C_{60}^{-}) distances of 2.28–2.32 Å and the Co atom deviates from the plane of the porphyrin macrocycle by 0.091(3) Å to 0.113(1) Å.[11] The TMP^{+} cation is located exactly above the Co atom (Figure 1, left). The shortest Co···P distance is 4.069 Å.

DABCO is a strongly coordinating bidentate ligand. The addition of one equivalent of CH_3I to DABCO affords a coordinating monodentate $MDABCO^+$ cation. The building block of **2** is similar to that of **1**. However, $MDABCO^+$ additionally coordinates to $Co^{II}OEP$ (the Co–N distance is 2.340(3) Å; Figure 1, right). This coordination weakens the Co•••C(C_{60}^-) bonding and the shortest Co•••C distance in **2** noticeably elongates to 2.508(4) Å at 100 K. The Co atom is more strongly bound to $MDABCO^+$ than to C_{60}^- and, as a result, is slightly shifted (0.042(1) Å) from the mean plane of the four porphyrin nitrogen atoms towards the nitrogen atom from $MDABCO^+$. The porphyrin macrocycle has the same concave conformation as in **1** with rms = 0.102 Å. The C_{60}^- anions are disordered in both **1** and **2** (see the Experimental Section) owing to their rotation about the coordination Co–C(C_{60}^-) bond. The coordinated carbon atoms under such disorder are ordered in both complexes in a way that allows the Co•••C(C_{60}^-) distances to be determined. Weaker Co–C(C_{60}^-) bonding in **2** provides a larger degree of C_{60}^- disorder. Indeed, there are three orientations of C_{60}^- in **2** with 0.4:0.3:0.3 occupancies and only two such orientations in **1** with 0.75:0.25 occupancies.

The fullerenes form zigzag one-dimensional chains along the *a* axis (Figure 2). The zigzag arrangement of the fullerenes produces cavities for small cations, which protrude into the fullerene chains. The center-to-center distances between C_{60}^- in the chains are 10.026 Å in **1** and 10.297 Å in **2**. The van der Waals interfullerene C–C contacts of 3.195–3.562 Å are observed only in **1**, whereas in **2** the larger $MDABCO^+$ cations force the C_{60}^- units apart from each other.

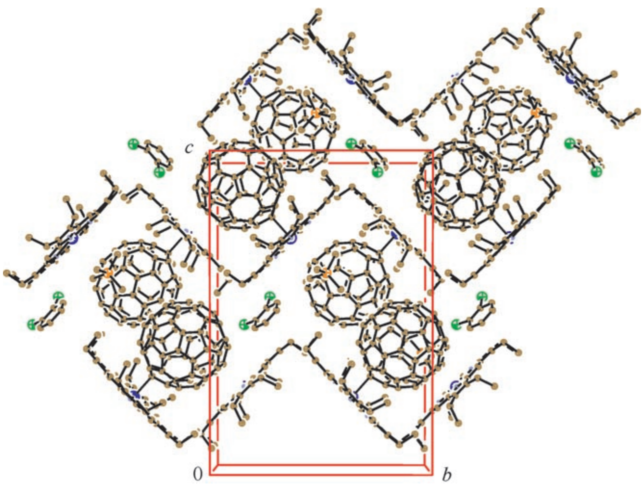

Figure 2. View of the crystal structure of **1** along the *a* axis and the fullerene zigzag chains. Only the major orientation of disordered C_{60}^- and the dichlorobenzene molecules is shown. Complex **2** has similar crystal packing.

Compound **1** is EPR silent at 290 K, whereas at low temperatures (4–120 K) two weak EPR signals are resolved. The signal with a *g* factor of 1.9996 and a line half-width (ΔH) of 0.48 mT at 4 K was attributed to isolated nonbonded $C_{60}^{\bullet-}$. This signal noticeably broadens with an increase of temperature, which is characteristic of $C_{60}^{\bullet-}$ radical anions.[15] A broad asymmetric signal with approximate *g* factors of 2.31 and 2.29 ($\Delta H \cong 60$ and 40 mT, respectively, at 4 K) was attributed to $Co^{II}OEP$. The estimated integral intensities of both signals did not exceed 2% of the total amount of $Co^{II}OEP$ and $C_{60}^{\bullet-}$. Therefore, **1** is EPR silent in the 4–290 K range, justifying the formation of diamagnetic σ-bonded {$Co^{II}OEP(C_{60}^-)$} units and in accordance with X-ray diffraction data. Weak EPR signals observed for **1** at low temperatures can be attributed to a small amount of EPR-active isolated $Co^{II}OEP$ and $C_{60}^{\bullet-}$ species retained in the sample in the nonbonded state. Similar residual EPR signals were observed in ionic fullerene complexes after $C_{60}^{\bullet-}$ and $C_{70}^{\bullet-}$ dimerization.[16]

Two weak EPR signals were also observed for **2** in the 4–50 K range. At 4 K the signal with $g = 1.9996$ and $\Delta H = 0.44$ mT was attributed to isolated nonbonded $C_{60}^{\bullet-}$ (this signal also noticeably broadens with the temperature increase to give $\Delta H = 4.64$ mT at 120 K), and an asymmetric signal with $g_1 = 2.3774$ and $g_2 = 2.3011$ ($\Delta H = 7.5$ and 14.5 mT) was attributed to $Co^{II}OEP$ coordinated to $MDABCO^+$. The total integral intensity of both signals was less than 2% of the total amount of C_{60}^- and $Co^{II}OEP$, and both signals could not be resolved above 140 K. The EPR data verify the diamagnetism of the {($MDABCO^+$)-$Co^{II}OEP(C_{60}^-)$} assemblies in **2** in the 4–50 K range due to the $Co^{II}OEP$ and $C_{60}^{\bullet-}$ spins pairing on formation of a Co–C(C_{60}^-) coordination σ bond. The broad signal reversibly grows above 50 K (Figure 3) and above 250 K its integral intensity corresponds to the contribution of about two $^1/_2$ spins per formula unit (both $Co^{II}OEP$ and $C_{60}^{\bullet-}$ have $^1/_2$ spin states). The signal has a *g* factor of 2.1188 ($\Delta H = 52$ mT) at room temperature, which is between those values characteristic of $Co^{II}OEP$ (the asymmetric signal with $g_1 = 2.37$, $g_2 = 2.03$ for five-coordinated $Co^{II}OEP$)[17] and $C_{60}^{\bullet-}$ ($g = 1.9996$–2.0000),[15] thus indicating strong exchange coupling between

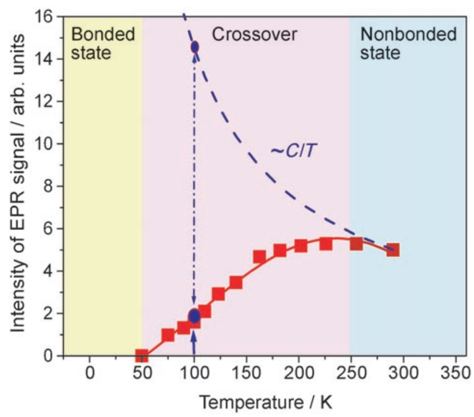

Figure 3. Temperature dependence of the integral intensity of the EPR signal in **2** (red curve) attributed to a resonating signal from nonbonded paramagnetic $Co^{II}OEP$ and $C_{60}^{\bullet-}$ species. The behavior is reversible. The blue dashed line shows the expected integral intensity of the EPR signal for noninteracting paramagnetic centers. The blue arrow indicates the temperature at which the crystal structure of **2** was determined, and the corresponding values of both the observed and expected integral intensities of the EPR signal (*C* is the Curie constant, *T* is temperature).

these paramagnetic species. Therefore, the Co–C(C_{60}^-) coordination σ bond observed at low temperatures completely dissociates above 250 K to produce two nonbonded paramagnetic {($MDABCO^+$)Co^{II}OEP} and $C_{60}^{\bullet-}$ species. This is the first example of such reversible formation of the Co–C-(C_{60}^-) bond, which resulted in the transition from a paramagnetic to a diamagnetic state.

The IR spectra of **1** and **2** indicate the ionic ground state of the complexes (see the Experimental Section). The $F_{1u}(4)$ mode of C_{60}, which is sensitive to charge transfer (CT) to the fullerene molecule,[18] is shifted from $\tilde{\nu} = 1429\ cm^{-1}$ to 1387, 1395, and 1398 cm^{-1} (split band) in **1** and to 1378, 1387, and 1394 cm^{-1} (split band) in **2**. The difference in the bonding in **1** and **2** at 290 K is seen in their NIR spectra (Figure 4). The bands of the nonbonded $C_{60}^{\bullet-}$ radical anion

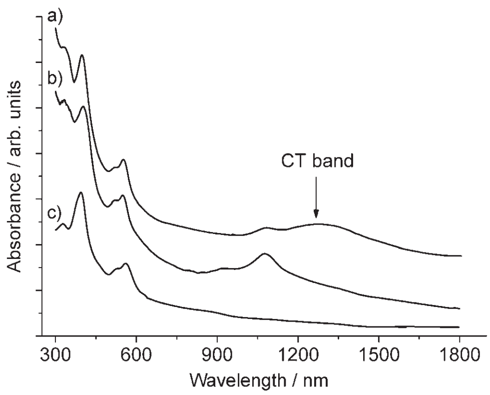

Figure 4. UV-visible-NIR spectra of a) **1**, b) **2**, and c) pristine Co^{II}OEP in KBr pellets.

are mainly observed in the spectrum of **2** at $\lambda = 933$ and 1078 nm (these two bands are characteristic of $C_{60}^{\bullet-}$ and were previously observed in salts and ionic complexes containing $C_{60}^{\bullet-}$ radical ions[15]). On the contrary, in the spectrum of **1** the band of $C_{60}^{\bullet-}$ at $\lambda = 1086$ nm decreases in intensity and a strong, broad band manifests itself at 1277 nm. The first band was attributed to the intramolecular transitions in the bonded C_{60}^- anion, whereas the second band can be attributed to CT between Co^{II}OEP and C_{60}^-. Previously, similar CT bands with slightly different positions were observed in multicomponent complexes containing σ-bonded diamagnetic {Co^{II}TPP(fullerene$^-$)} units.[11,19] Coordination noticeably shifts the positions of the Soret and the Q bands of Co^{II}OEP. Pristine Co^{II}OEP has bands at $\lambda = 394$, 531, and 560 nm and these bands appear at $\lambda = 398$, 523, and 552 nm and at $\lambda = 402$, 522, and 549 nm in the spectra of **1** and **2**, respectively. Therefore, the Soret band is redshifted by up to 8 nm and the Q bands are blueshifted by 8 to 11 nm.

Conclusion

The preparation of new, ionic, multicomponent complexes **1** and **2** has allowed, for the first time, the study of the coordination of C_{60}^- anions to cobalt(II) octaethylporphyrin. Noncoordinating TMP^+ cations provide the formation of stable σ-bonded diamagnetic {Co^{II}OEP(C_{60}^-)} units, which are similar to the previously described {Co^{II}TPP(C_{60}^-)} units.[11] In contrast to TMP^+, $MDABCO^+$ cations additionally coordinate to Co^{II}OEP to destabilize the Co–C(C_{60}^-) coordination bond. This bond reversibly dissociates in the 50–250 K range and this dissociation is accompanied by a diamagnetic–paramagnetic transition. TMP^+ and $MDABCO^+$ cations only differ in their coordination ability, which results in different degrees of Co^{II}OEP–(C_{60}^-) bonding, and different magnetic and optical properties of **1** and **2**. Therefore, these parameters can be controlled in the multicomponent complexes by choosing the cation type. The crystal structure of **2** was determined at 100 K, when the Co–C(C_{60}^-) coordination σ bond with a length of 2.508(4) Å is formed (according to EPR, the contribution of a diamagnetic bonded state in {($MDABCO^+$)Co^{II}OEP(C_{60}^-)} assemblies is about 90% at 100 K (Figure 3)). Thus, the Co···C distance of about 2.51 Å can be considered as a limiting length for the Co–C(C_{60}^-) coordination σ bond. This bond length is longer than the strong Co–C bond in alkylcobalamins (1.99–2.03 Å[8]) and the Co–C bond in **1** (2.27 Å).

Experimental Section

Materials: Cobalt(II) octaethylporphyrin (Co^{II}OEP), diazabicyclooctane (DABCO), sodium ethanethiolate (CH_3CH_2SNa), tetramethylphosphonium chloride (TMPCl), and methyl iodide (CH_3I) were purchased from Aldrich, and C_{60} (99.98% purity) was purchased from MTR Ltd. The solvents were purified in an argon atmosphere. *o*-Dichlorobenzene ($C_6H_4Cl_2$) was distilled over CaH_2, P_2O_5, and K_2CO_3 under reduced pressure, benzonitrile (C_6H_5CN) was distilled over Na under reduced pressure, and hexane and benzene were distilled over Na/benzophenone. The solvents were degassed and stored in a glove box. All manipulations for the synthesis of air-sensitive **1** and **2** were carried out in a MBraun 150B-G glove box with a controlled atmosphere and with an H_2O and O_2 content of less than 1 ppm. The crystals were stored in a glove box and were sealed in 2 mm quarts tubes for EPR measurements under 10^{-5} torr. KBr pellets for the IR and UV-visible-NIR measurements were prepared in a glove box.

General: UV-visible-NIR spectra were measured on a Shimadzu-3100 spectrometer in the $\lambda = 240$–2600 nm range. FTIR spectra were measured by using KBr pellets with a Perkin–Elmer 1000 Series spectrometer ($\tilde{\nu} =$ 400–7800 cm^{-1}). EPR spectra were recorded from 290 K down to 4 K and back from 4 K up to 290 K with a JEOL JES-TE 200 X-band ESR spectrometer equipped with a JEOL ES-CT470 cryostat. The integral intensity of the signals from a weighed amount of **1** and **2** was calibrated by the comparison with the integral intensity of the EPR signal from a weighed amount of $CuSO_4 \cdot 5H_2O$.

Synthesis: *N*-Methyldiazabicyclooctane iodide (MDABCOI) was obtained by the dropwise addition of one molar equivalent of CH_3I (1.11 mL, 0.0178 mol) to DABCO (2 g, 0.0178 mol) dissolved in hexane (60 mL) while stirring. A white crystalline precipitate of MDABCOI formed during the addition. After 1 h the precipitate was filtered off, washed with hexane (100 mL), and dried under vacuum over 8 h.

MDABCOI (4.07 g, 90%) was obtained with a satisfactory elemental analysis.

The crystals of **1** were obtained by the following procedure: C_{60} (25 mg, 0.035 mmol), a 10-fold molar excess of CH_3CH_2SNa (30 mg, 0.35 mmol), and a 5-fold molar excess of TMPCl (22 mg, 0.175 mmol) were stirred in a $C_6H_4Cl_2/C_6H_5CN$ (19:1; 20 mL) mixture for 1 h at 60°C. C_6H_5CN was added to increase the solubility of CH_3CH_2SNa and TMPCl, which are very poorly soluble in pure $C_6H_4Cl_2$. During stirring, the solution changed from violet, characteristic of neutral C_{60}, to red-brown. After cooling the solution down to room temperature and filtering it, the NIR spectrum of the solution was measured to indicate the selective reduction of C_{60} to the monoanionic state. Co^{II}OEP (21 mg, 0.035 mmol) was dissolved in the solution at 60°C for 1 h. The resulting solution was cooled, filtered into a glass tube (1.8 cm diameter, 50 mL volume) with a ground glass plug, and hexane (20 mL) was layered over the solution. The diffusion was carried out over 2 months to give crystals of **1** on the wall of the tube. The solvent was decanted from the crystals and they were washed with hexane to give black prisms with a characteristic blue luster (up to $0.3\times0.5\times1$ mm^3 in size) in 20% yield.

Table 1. X-ray diffraction data for **1** and **2**.

	1	**2**
structural formula	$[(TMP^+)\{Co^{II}OEP(C_{60}^-)\}$-$(C_6H_5CN)_{0.75}(C_6H_4Cl_2)_{0.25}]$	$[\{(MDABCO^+)Co^{II}OEP(C_{60}^-)\}$-$(C_6H_5CN)_{0.67}(C_6H_4Cl_2)_{0.33}]$
empirical formula	$C_{106.75}H_{60.75}N_{4.75}Cl_{0.5}PCo$	$C_{109.68}H_{63.67}N_{6.67}Cl_{0.66}Co$
M_r [g mol^{-1}]	1517.48	1557.15
color, shape	black, prisms	black, prisms
size [mm]	$0.50\times0.30\times0.20$	$0.40\times0.20\times0.20$
system	orthorhombic	orthorhombic
space group	$P2_12_12_1$	$Pna2_1$
a [Å]	14.9130(5)	26.1193(9)
b [Å]	17.7736(6)	17.9102(6)
c [Å]	25.8503(8)	14.9018(5)
V [Å^3]	6851.8(4)	6971.1(4)
Z	4	4
ρ_{calcd} [g cm^{-3}]	1.471	1.484
μ [mm^{-1}]	0.357	0.338
$F(000)$	3140	3227
max/min transmission	0.84/0.93	0.88/0.93
T [K]	100 (2)	100 (2)
max 2θ [°]	65.2	56.56
reflns measured	62958	43541
unique reflns	24435	13559
parameters	1601	1652
restraints	1640	9918
reflns [$F_o>2\sigma F_o$]	19220	10783
R_1 [$F_o>2\sigma F_o$]	0.0496	0.0769
wR_2 (all data)[a]	0.1162	0.1690
a	0.0683	0.1060
b	1.2556	2219.48
GOF	1.040	1.070
restr. GOF	1.018	1.063

[a] $w=1/[\sigma^2(F_o^2)+(aP)^2+bP]$, $P=[\max(F_o^2,0)+2F_c^2]/3$.

A similar procedure was used for the preparation of **2**. After cooling the solution with dissolved Co^{II}OEP, a polycrystalline precipitate of **2** formed over several hours. The small crystals suitable for X-ray diffraction measurements were obtained by the diffusion of a solution of Co^{II}OEP (16 mg, 0.027 mmol) in hexane/benzene (4:1, 25 mL) into a $C_6H_4Cl_2/C_6H_5CN$ solution (19:1; 20 mL) obtained from the reduction of C_{60} (25 mg, 0.035 mmol) by a 10-fold molar excess of CH_3CH_3SNa (30 mg, 0.35 mmol) in the presence of a 5-fold molar excess of MDABCOI (44.5 mg, 0.175 mmol). After 2 months, small crystals of **2** formed on the wall of the tube. The solvent was decanted from the crystals, which were washed with hexane to give small parallelepipeds with a characteristic blue luster (up to $0.2\times0.2\times0.4$ mm^3 in size) in 30% yield.

$[(TMP^+)\{Co^{II}OEP(C_{60}^-)\}(C_6H_5CN)_{0.75}(C_6H_4Cl_2)_{0.25}]$ (1): Elemental analysis calcd (%) for $C_{106.75}H_{60.75}N_{4.75}O_2Cl_{0.5}PCo$ (1549.48): C 82.65, H 3.95, N 4.32, O 2.08, Cl 1.15, P 2.01; found: C 81.34, H 3.51, N 3.56, Cl 1.12, P 2.31.

$[\{(MDABCO^+)Co^{II}OEP(C_{60}^-)\}(C_6H_5CN)_{0.67}(C_6H_4Cl_2)_{0.33}]$ (2): Elemental analysis calcd (%) for $C_{109.68}H_{63.67}N_{6.67}O_2Cl_{0.66}Co$ (1589.15): C 82.92, H 4.00, N 5.88, O 2.01, Cl 1.48; found: C 82.22, H 3.92, N 5.72, Cl 1.74.

The compositions of **1** and **2** were determined from the elemental analysis, and were verified by X-ray diffraction analysis on a single crystal. The difference between the value calculated by using the equation [100−(C, H, N, Cl, P,)]% and the calculated content of Co for air-sensitive **1** and **2** indicates the addition of oxygen to the complex in the course of the analysis (about one O_2 molecule per formula unit). The addition of O_2 to ionic C_{60} complexes during the elemental analysis has also been reported elsewhere.[16,20,21]

Crystal-structure determination: X-ray diffraction data for **1** and **2** were collected at 100(2) K by using a Bruker Nonius X8 Apex diffractometer with CCD area detector ($Mo_{K\alpha}$ radiation, $\lambda=0.71073$ Å) equipped with an Oxford Cryosystems nitrogen gas-flow apparatus. The data were collected by ϕ and ω scans with a 0.3° frame width and 30 s exposure time per frame. The data were integrated, scaled, sorted, and averaged by using the Bruker AXS software package.[22] The structure was solved by direct methods using SHELXTL version 6.12.[22] The structure was refined by using full-matrix least-squares methods against F^2. No absorption corrections were performed for either complex. Non-hydrogen atoms were refined in the anisotropic approximation. Positions of the hydrogen atoms were calculated geometrically. Subsequently, the positions of the H atoms were refined by the "riding" model with $U_{iso}=1.2U_{eq}$ of the connected non-hydrogen atom or as ideal CH_3 groups with $U_{iso}=1.5U_{eq}$. The details of the crystal-structure analysis are given in Table 1.

Molecule disorder in 1 and 2: Co^{II}OEP and TMP^+ are ordered in **1** at 100 K. The C_{60}^- anions are disordered between two orientations (0.75:0.25 occupancies) related to the rotation of C_{60}^- by ≈15° about the Co−C(C_{60}^-) coordination bond and, correspondingly, the axis passing through the coordinated carbon atom and the carbon atom located opposite the coordinated carbon. Thus, these two carbon atoms are ordered in **1** in such a way that allows the Co···C(C_{60}^-) distance to be determined. Solvent C_6H_5CN and $C_6H_4Cl_2$ molecules share one position with 0.75:0.25 occupancies. Both molecules are disordered between two orientations and have 0.50:0.25 and 0.20:0.05 occupancies, respectively. In **2** only Co^{II}OEP is ordered at 100 K. The C_{60}^- disorder has been approximated by three restrained molecules of fullerene C_{60} with one collective carbon atom coordinating to the Co atom of Co^{II}OEP, the disorder being a distribution in three orientations with 0.4:0.3:0.3 occupancies given by the rotation about the Co−C(C_{60}^-) coordination bond. As a result, the carbon atom of C_{60}^- coordinated to Co^{II}OEP in **2** is ordered in such a way that also allows the Co···C(C_{60}^-) distance to be determined. $MDABCO^+$ cations are disordered in **2** between two orientations (0.56:0.44 occupancy) linked by the 20° rotation about the axis passing through two nitrogen atoms of $MDABCO^+$. C_6H_5CN and $C_6H_4Cl_2$ solvent molecules also share one position with 0.67:0.33 occupancies. Both molecules are disordered between two orientations and have 0.39:0.28 and 0.17:0.16 occupancies, respectively.

CCDC-291006 and 291007 contain the supplementary crystallographic data for compounds **2** and **1**, respectively. These data can be obtained free of charge from The Cambridge Crystallographic Data Center via www.ccdc.cam.uk.data_request/cif.

Acknowledgements

This work was partly supported by the Grant-in-Aid Scientific Research from the Ministry of Education, Culture, Sports, Science and Technology, Japan (152005019 and COEPROGRAMS), the RFBR (grant N 06-03-32824a), the Russian Science Support Foundation, and INTAS YSF (05-109-4653).

[1] D. M. Guldi, *Chem. Soc. Rev.* **2002**, *31*, 22–36.
[2] D. Gust, T. A. Moore, A. L. Moore, *Acc. Chem. Res.* **2001**, *34*, 40–48.
[3] M. M. Olmstead, D. A. Costa, K. Maitra, B. C. Noll, S. L. Phillips, P. M. Van Calcar, A. L. Balch, *J. Am. Chem. Soc.* **1999**, *121*, 7090–7097.
[4] D. R. Evans, N. L. P. Fackler, Z. Xie, C. E. F. Rickard, P. D. W. Boyd, C. A. Reed, *J. Am. Chem. Soc.* **1999**, *121*, 8466–8474.
[5] D. V. Konarev, I. S. Neretin, Yu. L. Slovokhotov, E. I. Yudanova, N. V. Drichko, Yu. M. Shul'ga, B. P. Tarasov, L. L. Gumanov, A. S. Batsanov, J. A. K. Howard, R. N. Lyubovskaya, *Chem. Eur. J.* **2001**, *7*, 2605–2616.
[6] D. V. Konarev, A. Yu. Kovalevsky, X. Li, I. S. Neretin, A. L. Litvinov, N. V. Drichko, Yu. L. Slovokhotov, P. Coppens, R. N. Lyubovskaya, *Inorg. Chem.* **2002**, *41*, 3638–3646.
[7] P. D. W. Boyd, C. A. Reed, *Acc. Chem. Res.* **2005**, *38*, 235–242.
[8] M. Rossi, J. P. Glusker, L. Randaccio, M. F. Summers, P. J. Toscano, L. G. Marzilli, *J. Am. Chem. Soc.* **1985**, *107*, 1729–1738.
[9] S. Stevenson, G. Rice, T. Glass, K. Harich, F. Cromer, M. R. Jordan, J. Craft, E. Hadju, R. Bible, M. M. Olmstead, K. Maitra, A. J. Fisher, A. L. Balch, H. C. Dorn, *Nature* **1999**, *401*, 55–57.
[10] M. M. Olmstead, A. Bettencourt-Dias, J. C. Duchamp, S. Stevenson, D. Marciu, H. C. Dorn, A. L. Balch, *Angew. Chem.* **2001**, *113*, 1263–1265; *Angew. Chem. Int. Ed.* **2001**, *40*, 1223–1225.
[11] D. V. Konarev, S. S. Khasanov, A. Otsuka, Y. Yoshida, R. N. Lyubovskaya, G. Saito, *Chem. Eur. J.* **2003**, *9*, 3837–3848.
[12] D. V. Konarev, I. S. Neretin, G. Saito, Yu. L. Slovokhotov, A. Otsuka, R. N. Lyubovskaya, *Dalton Trans.* **2003**, 3886–3891.
[13] R. Subramanian, P. Boulas, M. N. Vijayashree, F. D'Souza, M. T. Jones, K. M. Kadish, *J. Chem. Soc. Chem. Commun.* **1994**, 1847–1848.
[14] E. Allard, L. Rivière, J. Delaunay, D. Dubois, J. Cousseau, *Tetrahedron Lett.* **1999**, *40*, 7223–7226.
[15] C. A. Reed, R. D. Bolskar, *Chem. Rev.* **2000**, *100*, 1075–1120.
[16] D. V. Konarev, S. S. Khasanov, G. Saito, A. Otsuka, Y. Yoshida, R. N. Lyubovskaya, *J. Am. Chem. Soc.* **2003**, *125*, 10074–10083.
[17] A. Ozarowski, H. M. Lee, A. L. Balch, *J. Am. Chem. Soc.* **2003**, *125*, 12606–12614.
[18] T. Picher, R. Winkler, H. Kuzmany, *Phys. Rev. B* **1994**, *49*, 15879–15889.
[19] D. V. Konarev, S. S. Khasanov, A. Otsuka, Y. Yoshida, G. Saito, *J. Am. Chem. Soc.* **2002**, *124*, 7648–7649.
[20] P.-M. Allemand, K. C. Khemani, A. Koch, F. Wudl, K. Holczer, S. Donovan, G. Grüner, J. D. Thompson, *Science* **1991**, *253*, 301–303.
[21] T. Kitagawa, Y. Lee, K. Takeuchi, *Chem. Commun.* **1999**, 1529–1530.
[22] Bruker Analytical X-ray Systems, Madison, Wisconsin (USA), **1999**.

Received: January 30, 2006
Published online: May 2, 2006

